JOURNAL OF VIROLOGY, Nov. 2005, p. 14017–14030 Vol. 79, No. 22
0022-538X/05/$08.00+0 doi:10.1128/JVI.79.22.14017–14030.2005


# The P Domain of Norovirus Capsid Protein Forms a Subviral Particle That Binds to Histo-Blood Group Antigen Receptors

Ming Tan and Xi Jiang*

*Division of Infectious Diseases, Cincinnati Children's Hospital Medical Center, and Department of Pediatrics, University of Cincinnati College of Medicine, Cincinnati, Ohio*

Received 24 May 2005/Accepted 11 August 2005

**Norovirus is the most important cause of nonbacterial acute gastroenteritis. We have shown previously that the isolated P domain containing the hinge forms a dimer and binds to histo-blood group antigen (HBGA) receptors with a low affinity (M. Tan, R. S. Hegde, and X. Jiang, J. Virol. 78:6233–6242, 2004). Here, we reported that the P domain of VA387 without the hinge forms a small particle with a significantly increased receptor binding affinity. An end-linked oligopeptide containing one or more cysteines promoted P-particle formation by forming intermolecular disulfide bridges. The binding sensitivity of the P particle to HBGAs was enhanced >700-fold compared to the P dimer, which was comparable to that of virus-like particles. The binding specificity of the P particle was further confirmed by strong binding to the Caco-2 cells, a human colon carcinoma cell line. This binding enhancement was observed in the P particles of both norovirus GI and GII strains. The P particle is estimated to contain 12 P dimers, in which the P2 subdomain builds up the outer layer, while the P1 subdomain forms the internal core. Taken together, our data indicate that the P domain is involved not only in dimerization but also in polymerization of the protein during the capsid assembling. The enhanced receptor binding of the P particle reflects the intrinsic feature of the viral capsid. The easy production of the P particle and its strong binding to HBGAs suggest that the P particle is useful in studying pathogenesis and morphogenesis of norovirus and candidates for antiviral or vaccine development.**

Norovirus, previously called Norwalk-like virus or small round structured virus, is the most important viral pathogen of epidemic acute gastroenteritis in both developed and developing countries (9, 10). Recent advances in understanding of norovirus-host interaction and the viral receptors have opened a new approach to study the host range and pathogenesis (18, 31). Noroviruses recognize human histo-blood group antigens (HBGAs) as receptors, which are complex carbohydrates present on red blood cells and mucosal epithelium or as free antigens in biological fluids, such as saliva, milk, and intestinal contents (25, 29). The recognition of HBGAs by noroviruses is strain specific, and eight distinct receptor-binding patterns have been identified (13, 14, 16, 17, 19, 26). The linkage of norovirus binding to HBGAs with clinical infection has been demonstrated in human volunteer studies. In the case of the prototype Norwalk virus (NV), for example, individuals of nonsecretors were naturally resistant to NV infection following the challenge (23). It seems logical to predict that each virus strain of the other binding patterns has its own host range defined by host blood type, although a recent human volunteer study of another norovirus, the Snow Mountain virus, did not reveal clear association between infection and host blood type (22).

Norovirus belongs to the family *Caliciviridae*. It contains a positive-strand, polyadenylated RNA genome of ~7.7 kb that is encompassed by a protein capsid. The viral capsid is composed of a single major structural protein forming an icosahedral particle that is believed to have many important functions, such as host-receptor interaction and host immune recognition. Biological characterization of human noroviruses has been hampered by the lack of an in vitro culture and an animal model for propagation of the viruses. The successful expression of norovirus capsid proteins and the fact that the capsid proteins spontaneously form virus-like particles (VLPs) provided valuable materials for studying norovirus in many aspects of immunology, epidemiology, and pathogenesis (16, 17, 21).

The atomic structure of the recombinant NV capsid indicated that norovirus capsid contains 180 capsid protein monomers organized into 90 dimeric capsomers that form a T=3 icosahedron (28). Each of the capsid protein is composed of two major domains, the N-terminal shell (S) and the C-terminal protrusion (P) domains, linked by an eight-amino-acid hinge. The S domain folds in an eight-stranded β-barrel that commonly occurs in the capsid proteins of other viral families and forms the contiguous shell of the capsid. The P domain builds up the arch-like structures extending from the shell. Morphogenesis studies showed that the S domain is required for the assembly of the capsid (2) and participates in multiple intermolecular interactions of dimers and pentamers of dimers, whereas the P domain is involved in dimeric interaction (28). It has been shown that the isolated P domains with the hinge form dimers in vitro that maintain binding function to HBGA receptors (32). The P domain can be further divided into P1 and P2 subdomains, which correspond to the leg and the top of the arch-like capsomer, respectively (28). Because the P2 subdomain contains the most variable sequence and is located on the surface of the capsid, it has been assumed that the P2 subdomain is critical for host immune and receptor interactions. Indeed, a binding interface has been identified in this region by computer modeling, followed by site-directed mutagenesis analysis (3, 20, 33).

* Corresponding author. Mailing address: Division of Infectious Diseases, Cincinnati Children's Hospital Medical Center, 3333 Burnet Ave., Cincinnati, OH 45229-3039. Phone: (513) 636-0119. Fax: (513) 636-7655. E-mail: jason.jiang@cchmc.org.

Sequence analysis of norovirus capsid protein showed that there are many trypsin and chymotripsin cleavage sites across the entire protein. However, proteolytic analysis of the norovirus VLPs resulted in only partial digestion of the capsid protein, in which the S domain was completely digested, while the P domain remained intact when the NV VLPs were treated with trypsin (12). Partial digestion of NV capsid protein was also observed when the recombinant NV capsid protein was expressed in baculovirus (21). More interestingly, a large amount of soluble 30-kDa norovirus protein was found in stools of NV-infected patients (11); this soluble protein was later demonstrated to be the P domain of the capsid protein (12). N-terminal sequencing of the NV-soluble P protein showed that it begins at $T_{227}$ of the NV capsid protein, which is the third amino acid of the P domain (12). These data indicate that the P domain must have folded in certain structures that are resistant to proteases. The survival of the P protein through the human intestinal tract suggests that the P domain possesses some biological functions.

In the current study, we further characterized the norovirus P domain by biochemical and mutagenesis approaches. We demonstrated that, when expressed in *Escherichia coli*, the P domain without the hinge forms a complex (P particle) that displays enhanced binding ability to HBGAs. This differs from the previous observation that the P protein containing the hinge forms a dimer and has a lower binding affinity to HBGAs (32). We also showed that the P particle is composed of 12 identical P dimers that organized most likely into a T=1 icosahedron. The mechanism and factors that affect the intermolecular interactions and the stability of the P particles are discussed.

## MATERIALS AND METHODS

**Construction of norovirus capsid protein mutants.** Various mutants of VA387 and NV capsid proteins used in this study were constructed by cloning the full-length or partial capsid genes into pFastBac (Bac-to-Bac Baculovirus Expression system; Invitrogen, Carlsbad, CA) at the BamHI and NotI sites for expression in baculovirus or into pGEX-4T-1 (GST Gene Fusion system; Amersham Biosciences, Piscataway, NJ) at the BamHI and NotI sites for expression in bacteria. All mutants with N- or C-terminal-linked short peptides were prepared with primers with the peptide-encoding sequences at their 5′ or 3′ ends (Table 1). The mutant of VA387 capsid protein with a $T_{338}A$ mutation was constructed using the QuickChange site-directed mutagenesis kit (Stratagene, La Jolla, CA) as previously described (33). The mutants CNGRCTTDC-H/P and CVQPCNGRC-H/P were made from the construct CNGRC-H/P by mutagenesis using the same QuickChange site-directed mutagenesis kit. The construct for expressing CNGRC-MBP (maltose-binding protein) was made by amplifying the MBP-encoding sequence from the plasmid pMALc2 (NEB, Hercules, CA), in which the forward primer contained the CNGRC-encoding sequence. The mutation sites and cloning conjunctions of all expression constructs were confirmed by sequencing. Table 1 lists all primers used in this study.

**Expression and purification of norovirus VLPs.** The capsid proteins of NV and VA387, representing the norovirus genogroups I and II, respectively, were expressed in insect cell *Spodoptera frugiperda* (Sf9) using the Bac-to-Bac baculovirus expression system (Invitrogen, Carlsbad, CA) as described previously (16). Briefly, the cDNA sequences of open reading frames 2 and 3 were cloned into pFastBac donor plasmid and transposed into bacmid. Sf9 cells were then infected with the recombinant bacmid containing the capsid genes. The VLPs from the infected insect cells were partially purified by centrifugation through a sucrose gradient containing 10% to 50% sucrose. The peak fractions containing VLPs were pooled and stored at −70°C in phosphate-buffered saline (PBS), pH 7.4.

**Expression and purification of the recombinant P proteins in *E. coli*.** After sequence confirmation, the constructs containing different norovirus P protein-encoding sequences were expressed in *E. coli* strain BL21 at room temperature overnight with an induction of 0.5 mM IPTG (isopropyl-β-D-thiogalactopyranoside). Purification of the recombinant glutathione *S*-transferase (GST)-P fusion protein from bacteria was performed with Glutathione Sepharose 4 Fast Flow (Amersham Biosciences, Piscataway, NJ) according to the manufacturer's instructions, as described previously (32, 34). The fusion protein was eluted by glutathione (Amersham Biosciences, Piscataway, NJ), and the P proteins were released from GST by thrombin (Amersham Biosciences, Piscataway, NJ) cleavage at room temperature for 16 h. Further purification was conducted by gel filtration using a size exclusion column and/or anion exchange (see below). Protein concentrations were measured spectroscopically or by quantitative sodium dodecyl sulfate-polyacrylamide gel electrophoresis (SDS-PAGE), depending on the purity of the proteins.

**Gel filtration.** To further purify the capsid proteins and/or to measure the molecular weight of the proteins, the affinity column-purified proteins were loaded on the size exclusion column Superdex 200 (Amersham Biosciences, Piscataway, NJ), powered by an AKTA fast-performance liquid chromatography (FPLC) system (model 920; Amersham Biosciences, Piscataway, NJ). The proteins of each peak were analyzed by SDS-PAGE and/or Western analysis. The molecular weight of the proteins in each fraction was calibrated with the Gel Filtration Calibration kit (Amersham Biosciences, Piscataway, NJ). Gel filtrations were run using PBS, pH 7.4, except as otherwise indicated.

**Anion-exchange chromatography.** The anion-exchange system Q Sepharose High Performance (Amersham Biosciences, Piscataway, NJ) was packed in a Flex column with a flow adapter (Kontes, Vineland, NJ) powered by an AKTA FPLC System (model 920; Amersham Biosciences, Piscataway, NJ). The P proteins purified by affinity column or gel filtration were adsorbed to the anion exchanger in binding buffer (20 mM Tris-HCl, pH 8.0). The proteins were then eluted by an increasing salt gradient of elution buffer (1 M NaCl, 20 mM Tris-HCl, pH 8.0). The proteins of each peak were analyzed by SDS-PAGE and/or Western analysis.

**Nondenatured and nonreduced PAGE.** To demonstrate the existence of the P particles, the P proteins were loaded onto a nondenatured polyacrylamide gel without boiling the proteins by using a loading buffer without SDS and reducing reagent. The nondenatured polyacrylamide gel was prepared and electrophoresed without SDS. The P protein known to form dimer only was used in the PAGE for a comparison.

**Assay of capsid proteins binding to HBGAs.** The binding capabilities of wild-type and mutant capsid proteins to HBGAs were measured by saliva-binding assays described previously (16). The blood types of the saliva donors whose saliva were used in this study were determined in a previous study (16). Synthetic oligosaccharides (Glycorex B, Lund, Sweden) were used as control to ensure that it was the HBGAs, not other components in the saliva, that reacted with the capsid proteins.

**Quantitative measurement of norovirus capsid proteins binding to HBGAs.** To compare the receptor-binding capabilities of the capsid proteins in different forms, the binding sensitivity of the VLP, the P dimer, and the P particle were determined by an end point titration by the standard saliva-binding assays (16, 32) with a cutoff point of an optical density at 450 nm of $\geq$0.1. For direct comparison, all recombinant capsid proteins were adjusted to a starting concentration of 1 mg/ml. Baculovirus-expressed VLPs of VA387 were included in each plate as an internal standard.

**Dissociation of VLPs.** To determine the role of the structural integrity of VLP in the receptor binding, we compared the binding activities of VLPs with their dissociated forms following a dissociation treatment of the VLPs. In one condition, VLPs were partially dissociated by dialyzing VLPs with 50 mM Tris (pH 9.0) for 3 to 6 h at room temperature (36). Alternatively, VLPs in the peak fractions (containing ~30% sucrose) of sucrose gradient were adjusted to contain 50 mM of Tris (pH 9.0) and then incubated at 4°C for 3 to 6 h. The treated VLPs were then analyzed by gel filtration as described previously. Fractions containing the intact VLPs and dissociated capsid proteins were assayed for receptor-binding abilities after they were adjusted to the same protein concentration with Centricon (Millipore, Danvers, MA).

**EM.** Gel filtration-purified P particles were prepared for electron microscopy (EM) examination using 1% ammonium molybdate as the staining solution (2). Specimens were examined under an EM10 C2 microscope (Zeiss, Germany) at 80 kV at a magnification of ×80,000.

**Mass spectrometry.** The molecular weights of the P-protein monomer and dimer were determined by electrospray ionization-mass spectrometry (MS) and by matrix-assisted laser desorption/ionization-MS (MALDI-MS) performed by the core facility at the University of Cincinnati, Cincinnati, Ohio. For electrospray ionization-MS, the P proteins were diluted in 50% acetonitrile–water–0.1% formic acid buffer and analyzed through a Micromass Q-TOF II mass spectrometer (Waters Corporation Milford, MA). The sample was directly infused through the instrument with a syringe pump. MALDI-MS was performed by

TABLE 1. Primers used to generate constructs for expression of recombinant capsid proteins[a]

| Name | Sequence (5′ to 3′) | Sense | Enzyme | Construct generated |
|---|---|---|---|---|
| P502 | GCACGGATCCATGAAGATGGCGTCGAATGAC | + | BamHI | F (full-length) |
| P423 | GGACGCGGCCGCTTATAATGCACGTCTGCGCCC | − | NotI | F, H/P, and P related |
| P422 | GCACGGATCCTTCTTGGTGCCACCCACAGTT | + | BamHI | H/P |
| P524 | GCACGGATCCTCAAGAACTAAACCATTCACC | + | BamHI | P |
| P517 | CCGCGTGGATCCTGCAACGGCCGTTGCTTCTTGGTGCCACC | + | BamHI | CNGRC-H/P |
| P518 | GGTGGCACCAAGAAGCAACGGCCGTTGCAGGATCCACGCGG | − | BamHI | CNGRC-H/P |
| P552 | GCAACGGCCGTTGCACGACTGATGGCTTCTTGGTGCCACC | + | | CNGRCTTDC-H/P |
| P553 | GGTGGCACCAAGAAGCCATCAGTCGTGCAACGGCCGTTGC | − | | CNGRCTTDC-H/P |
| P554 | GCGTGGATCCTGCGTCCAACCACAAAACGGCCGTTGCT | + | | CVQPQNGRC-H/P |
| P555 | AGCAACGGCCGTTTTGTGGTTGGACGCAGGATCCACGC | − | | CVQPQNGRC-H/P |
| P562 | GCACGGATCCCAAAATGGCAGGCCACCCACAGTTGAATCAAG | + | BamHI | QNGR-H/P |
| P563 | CGTGCGGCCGCTTAGCACCTGCCATTGCATAATGCACGTCTGCGCCCCGC | − | NotI | H/P-CNGRC, |
| P564 | GCGTGCGGCCGCTTAGCACCTGCCATTTTGGCATAATGCACGTCTGCGCCCCGC | − | NotI | H/P-CNGRC F-CQNGRC |
| P565 | GCACGGATCCTGCAATGGCAGGTGCGCGTCGAATGACGCCAGCCC | + | BamHI | CNGRC-F |
| P566 | GCACGGATCCTGCCAAAATGGCAGGTGCGCGTCGAATGACGCCAGCCC | + | BamHI | CQNGRC-F |
| P585 | GCGTGGATCCTGCAACGGCCGTTGCTTCTTGGTGCCACCCACAGTT | + | BamHI | CNGRC-H/P |
| P586 | GCGTGGATCCTGCGGAGGCGGTTGCTTCTTGGTGCCACCCACAGTT | + | BamHI | CGGGC-H/P |
| P589 | GCGTGGATCCAACGGCCGTTTCTTGGTGCCACCCACAGTT | + | BamHI | NGR-P |
| P590 | GCATGCGGCCGCTTAGCAAAAGCAATCGCCACGGCAATCGCATAATGCACGTCTGCGCCCCGC | − | NotI | P-CDCRGDCFC |
| P595 | AGTGCGGCCGCTTAGCAACCGCCTCCGCATAATGCACGTCTGCGCCCCGC | − | NotI | P-CGGGC |
| P596 | AGTGCGGCCGCTTAGCACGCGCCCGCGCATAATGCACGTCTGCGCCCCGC | − | NotI | P-CAGAC |
| P597 | AGTGCGGCCGCTTAGCAACGGCCGTTTAATGCACGTCTGCGCCCCGC | − | Not I | P-NGRC |
| P377 | GCTCACCCAAAACCGCAAGAGAGGATGGC | + | | CNGRC-H/P-T/A |
| P378 | GCCATCCTCTCTTGCGGTTTGGGTGAGC | − | | CNGRC-H/P-T/A |
| P493[b] | GCACGGATCCTTTTTAGTCCCTCCTACGGTG | + | BamHI | H/P |
| P494[b] | GGACGCGGCCGCTTATCGGCGCAGACCAAGCCT | − | NotI | H/P |
| P588[b] | GCGTGGATCCTGCAACGGCCGTTGCTTTTTAGTCCCTCCTACGGTG | + | BamHI | CNGRC-H/P |
| P649[b] | GCACGGATCCCAGAAAACCAGGCCCTTCACAC | + | BamHI | P |
| P583 | CACGGATCCTGCAATGGCAGCTGCAAAATCGAAGAAGGTAAACTGG | + | BamHI | CNGRC-MBP[c] |
| P584 | GCGTGCGGCCGCTTAAGTCTGCGCGTCTTTCATGGCTTC | − | Not I | CNGRC-MBP[c] |

[a] All sequences are strain VA387 except as otherwise noted. The enzyme recognition sites are underlined.
[b] Primers used for construction of Norwalk virus mutants.
[c] Constructs of maltose-binding proteins.

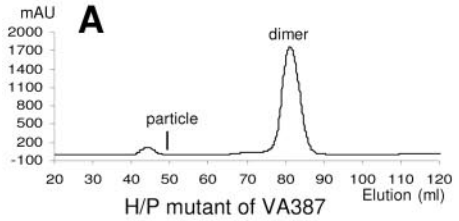
A
mAU
2000
1700
1400
1100
800
500
200
-100
particle
dimer
20 30 40 50 60 70 80 90 100 110 120
Elution (ml)
H/P mutant of VA387

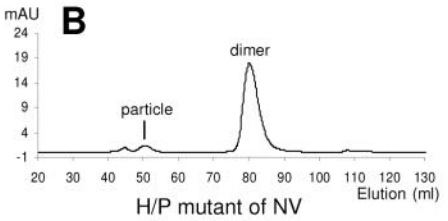
B
mAU
24
19
14
9
4
-1
particle
dimer
20 30 40 50 60 70 80 90 100 110 120 130
Elution (ml)
H/P mutant of NV

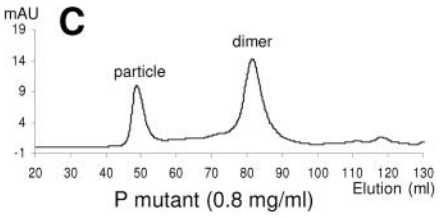
C
mAU
19
14
9
4
-1
particle
dimer
20 30 40 50 60 70 80 90 100 110 120 130
Elution (ml)
P mutant (0.8 mg/ml)

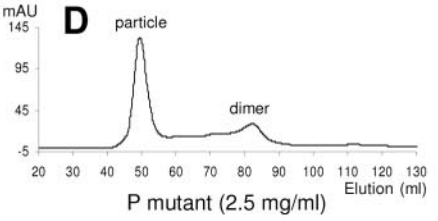
D
mAU
145
95
45
-5
particle
dimer
20 30 40 50 60 70 80 90 100 110 120 130
Elution (ml)
P mutant (2.5 mg/ml)


E
M 1 2 3
108
81
48
36
27
(kDa)

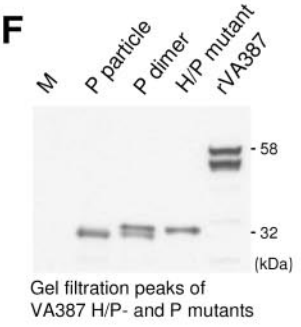
F
M
P particle
P dimer
H/P mutant
rVA387
58
32
(kDa)
Gel filtration peaks of
VA387 H/P- and P mutants

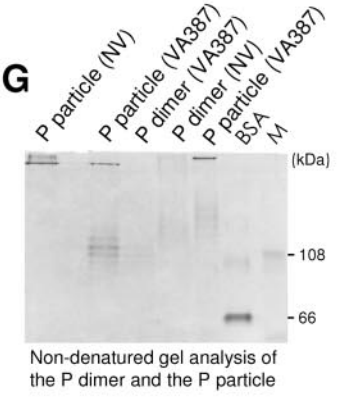
G
P particle (NV)
P particle (VA387)
P dimer (VA387)
P dimer (NV)
P particle (VA387)
BSA
M
(kDa)
108
66
Non-denatured gel analysis of
the P dimer and the P particle

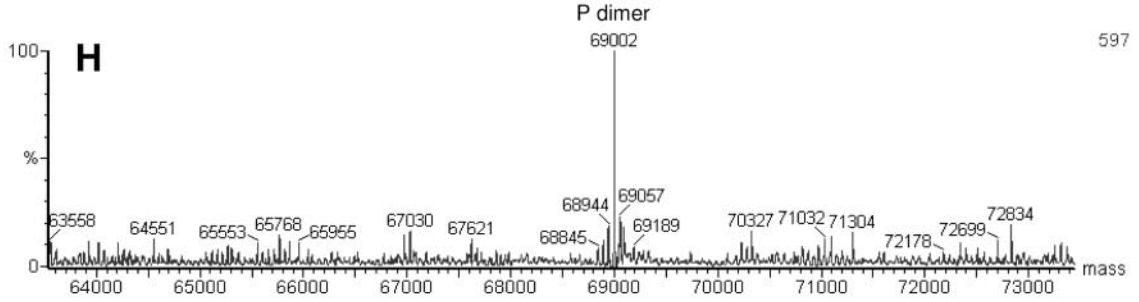
H
P dimer
69002
597
100
%
0
63558
64551
65553
65768
65955
67030
67621
68845
68944
69057
69189
70327
71032
71304
72178
72699
72834
mass
64000 65000 66000 67000 68000 69000 70000 71000 72000 73000

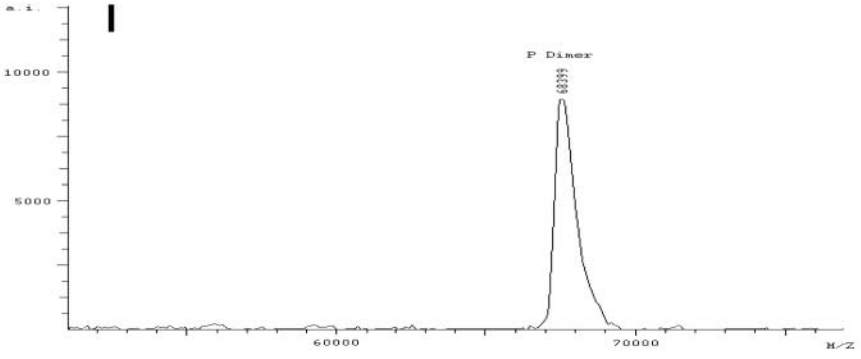
I
a.i.
10000
5000
P Dimer
60000
70000
M/Z

TABLE 2. Summary of the receptor-binding sensitivities of the P mutants and their abilities to form P particles

| Mutant[a] | Description | Dimer[b] | Multimer[b] | Binding sensitivity to HBGAs (ng/ml)[c] | | | |
|---|---|---|---|---|---|---|---|
| | | | | O | A | B | N |
| P domain | | | | | | | |
| P | P domain without hinge | Varied | Varied | 3,700[d] | 137.2[d] | 137.2[d] | $>10^5$[d] |
| H/P | P domain with hinge | >95% | <5% | $3 \times 10^4$ | 3,700 | 3,700 | $>10^5$ |
| NGR-H/P | H/P with NGR on N terminus | >99% | <1% | $>10^5$ | $>10^5$ | $>10^5$ | $>10^5$ |
| QNGR-H/P | H/P with QNGR on N terminus | >95% | <1% | $>10^5$ | 3,700 | 3,700 | $>10^5$ |
| H/P-NGRC | H/P with NGRC on C terminus | <15% | >85% | 411.5 | 15.3 | 5.1 | $>10^5$ |
| CGGGC-H/P | H/P with CGGGC on N terminus | <10% | >90% | 1,230 | 15.3 | 5.1 | $3 \times 10^4$ |
| CAGAC-H/P | H/P with CAGAC on N terminus | <10% | >90% | 1,230 | 15.3 | 5.1 | $>10^5$ |
| CNGRC-H/P | H/P with CNGRC on N terminus | <5% | >95% | 1,230 | 15.3 | 5.1 | $>10^5$ |
| H/P-CNGRC | H/P with CNGRC on C terminus | <5% | >95% | 1,230 | 15.3 | 5.1 | $>10^5$ |
| CNGRC-H/P-CNGRC | H/P with CNGRC on both ends | <5% | >95% | $3 \times 10^4$ | 15.3 | 15.3 | $>10^5$ |
| CVQPQNGRC-H/P | H/P with CVQPQNGRC on N terminus | <5% | >95% | 1,230 | 15.3 | 5.1 | $>10^5$ |
| CNGRCTTDC-H/P | H/P with CNGRCTTDC on N terminus | <5% | >95% | 3,700 | 15.3 | 5.1 | $>10^5$ |
| H/P-CDCRGDCFC | H/P with CDCRGDCFC on C terminus | <5% | >95% | 3,700 | 5.1 | 1.7 | $>10^5$ |
| GST-CNGRC-H/P | CNGRC-P/H with GST on N terminus | ND[f] | ND | $3 \times 10^4$ | 3,700 | 3,700 | $>10^5$ |
| P-NGRC | P with NGRC on C terminus | ~10%[e] | ~10%[e] | 411.5 | 15.3 | 5.1 | $>10^5$ |
| P-CGGGC | P with CGGGC on C terminus | <10% | >90% | 411.5 | 5.1 | 5.1 | $>10^5$ |
| H/P-T/A | H/P with mutation $T_{338}A$ | >95% | <5% | $>10^5$ | $>10^5$ | $>10^5$ | $>10^5$ |
| CNGRC-H/P-T/A | CNGRC-H/P with mutation $T_{338}A$ | <5% | >95% | $>10^5$ | $>10^5$ | $>10^5$ | $>10^5$ |
| CNGRC-MBP | MBP with CNGRC on N terminus | ND | ND | $>10^5$ | $>10^5$ | $>10^5$ | $>10^5$ |
| Full-length protein | | | | | | | |
| $F_{VLP}$ | Wild-type VLPs from insect cells | NA[g] | NA | 91.8 | 30.6 | 10.2 | $>10^5$ |
| H/P (NV) | P domain with hinge | >95% | <5% | 1,230 | 1,230 | $10^4$ | $>10^5$ |
| CNGRC-HP (NV) | H/P with CNGRC on N terminus | ~50% | ~50% | 45.7 | 15.2 | 1,230 | $>10^5$ |
| VLP (NV) | Wild-type VLPs from insect cells | NA | NA | 45.7 | 45.7 | 411.5 | $>10^5$ |

[a] All mutants are VA387 related except as otherwise noted.
[b] Formation of the P dimer or the P particle was determined by gel filtration using a size exclusion column, Superdex 200.
[c] The binding sensitivity was determined by saliva-binding assays using threefold series diluted recombinant capsid proteins. The values are the minimum protein concentrations that produce an optical density at 450 nm of 0.1 to 0.29. O, A, B, and N, saliva samples with blood types of O, A, B, and nonsecretor, respectively.
[d] Value that was measured using a fraction with protein concentration of 0.8 mg/ml.
[e] A total of 80% of this P protein was eluted in void volume.
[f] ND, not determined.
[g] NA, not applicable.

a standard protein analysis protocol using sinapinic acid as a matrix. The MALDI-MS was a Bruker Daltonics Reflex IV (Billerica, MA).

**Examination of the P particle binding to Caco-2 cells by fluorescence microscopy.** Caco-2 cells (a human colon carcinoma cell line) were cultivated using the conditions described by White et al. (35). The cells were maintained in the culture for 10 to 14 days postconfluency before being used for the binding assay. The P dimer (H/P) and the P particle (CNGRC-H/P), as well as a binding-defective mutant (PC-5) (M. Tan and X. Jiang, unpublished data), were biotinylated using the EZ-link biotinylation kit (Pierce, Rockford, IL). The labeled P proteins at indicated concentrations were incubated with the cells for 2 h at 37°C. After wash with Hank's balanced salt solution with $Mg^{2+}$ and $Ca^{2+}$ (Cambrex Bio Science, Walkersville, MD), fluorescein isothiocyanate-streptavidin (1:200; Pierce, Rockford, IL) was added to the cells and incubated for 60 min at 37°C. After a final wash with Hank's balanced salt solution, the cells were examined under a fluorescence microscope (Zeiss Axiovert S100; Germany) equipped with a SPOT digital camera (Diagnostic Instruments, Inc.).

## RESULTS

**The isolated P domain without the hinge forms a complex.** We reported previously that the isolated P domain with the hinge (H/P mutant) of noroviruses forms a dimer that binds to HBGAs (Fig. 1A and B) (32). Here, we show that the P domain without the hinge (P mutant) of VA387 formed a complex of dimers (P particle, see below) (Fig. 1C, D, F, and G). Gel filtration analysis using Superdex 200 showed that this

FIG. 1. The isolated P domain without the hinge forms P particles. (A to D) Chromatographs of gel filtrations of the H/P mutants (A and B) and the P mutants (C and D) of strains VA387 (A, C, and D) and NV (B), indicating peaks of the P dimer and the P particle. A minor peak in the void volume (~45 ml) sometimes occurred and contained proteins that did not react with norovirus-specific antibodies. The gel filtration column (Superdex 200; Amersham Biosciences) was calibrated by the calibration kit (Amersham Biosciences): 2,000 kDa, 44.3 ml (void); 669 kDa, 51.1 ml; 440 kDa, 56.2 ml; 232 kDa, 65.7 ml; 146 kDa, 70.8 ml; 67 kDa, 76.7 ml; 47 kDa, 82.7 ml; 25 kDa, 92.9 ml; and 13.7 kDa, 97.3 ml. (E) SDS-PAGE gel stained with brilliant blue (G250) to show P proteins of the P mutants purified by affinity column (lane 1) and by anion-exchange chromatography (lane 2), as well as the P protein of CNGRC-H/P mutant purified by affinity column, followed by anion-exchange chromatography (lane 3). (F) Western analysis of gel filtration peaks containing the P dimer and the P particle of VA387 with hyperimmune sera against the VLPs of VA387. (G) Nondenatured PAGE gel stained with brilliant blue (G250) to visualize the P particles as bands with high molecular masses. (H and I) Measurements of the molecular weight of the P dimer (P mutant) by electrospray ionization-MS (G) and by MALDI-MS (H).

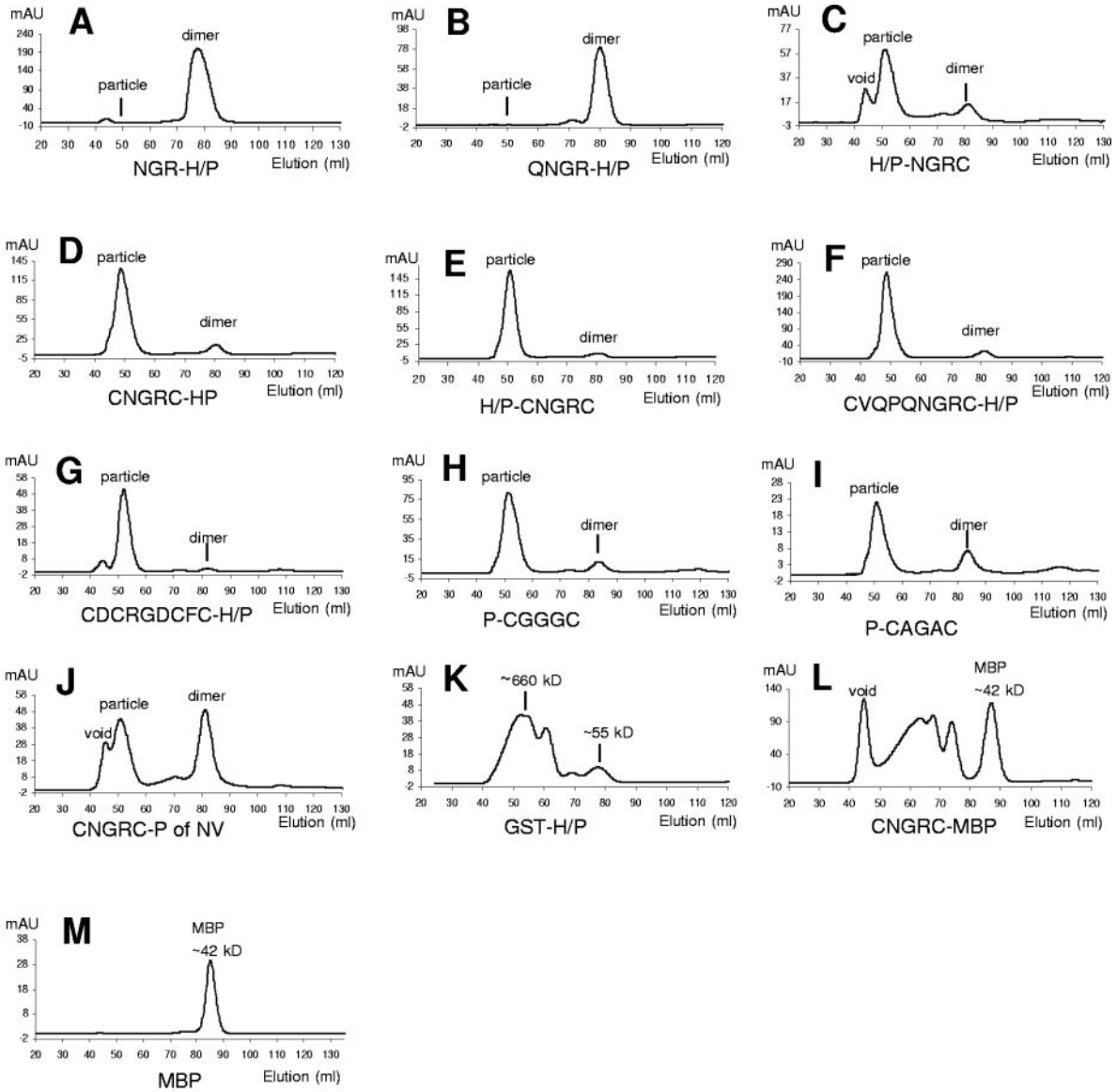


FIG. 2. An end-linked cysteine promotes the P particle formation. (A and B) H/P mutants with an N-terminus-fused short peptide without cysteine formed only P dimer. (C to J) Chromatographs of gel filtrations of P or H/P mutants with an end-linked cysteine-formed P particle. The minor peaks in the void volume (~45 ml) contained proteins unrelated to norovirus (Fig. 1). (K and L) Negative controls to demonstrate that the H/P mutant with GST (K) or MBP with the end-fused cysteines (L) did not form P particles. The gel filtration column was calibrated using the same calibration kit as described in the legend to Fig. 1.

complex was eluted at the same position as thyroglobilin, a protein standard with a molecular mass of 690 kDa (Amersham, Piscataway, NJ) (Fig. 1C and D), suggesting that this P complex contained 12 P dimers, as the P dimer was eluted at a position corresponding to 55 kDa (Fig. 1A and B) (32). Nondenatured PAGE confirmed the presence of the P particle as it appeared as a single high-molecular-mass protein band (Fig. 1G). There was no major contamination of the P protein following the affinity purification (Fig. 1E, lane 1). The P particle was further purified by anion-exchange chromatography (Fig. 1E, lane 2). The fact that only a single peak of the P particle and no intermediate product were seen in the gel filtration (Fig. 1C and D) suggests that the estimated 12 P dimers must be arranged in a low-energy order in the particle (see below). The formation of the P particle is P protein concentration dependent, as ~60% of the VA387 P mutant existed as dimers at a concentration of 0.8 mg/ml, whereas >90% of the P protein formed particles at 2.5 mg/ml (compare Fig. 1C and D). To accurately measure the molecular weights of the P dimer and the P particle, analytic mass spectrometry was performed. Both electrospray ionization-MS (Fig. 1H) and MALDI-MS (Fig. 1I) revealed a mass of ~69 kDa of the P dimer. Accordingly, the estimated molecular mass of the P particle (12 P dimers) should be ~830 kDa.

**An end-linked cysteine promotes P particle formation.** The fact that the P domain without the hinge formed P particles

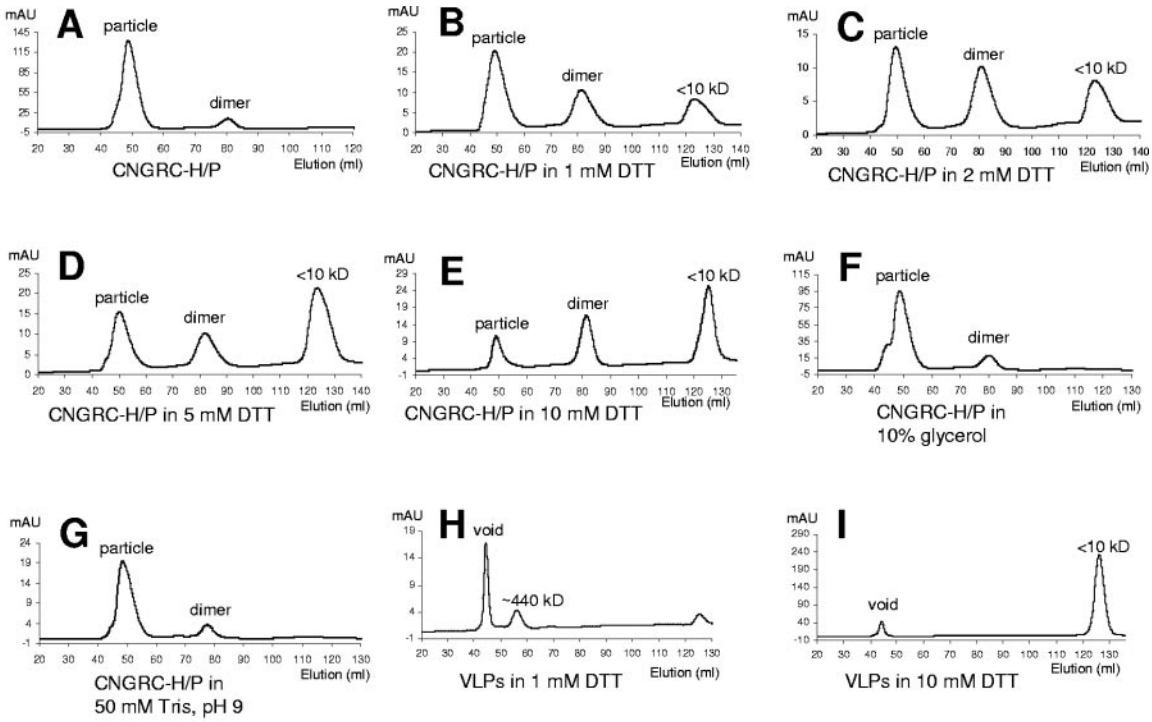


FIG. 3. The P particle and VLP of VA387 were dissociated by DTT. (A to E) Chromatographs of gel filtrations of the P particle of the CNGRC-H/P mutant (A) treated by 1 mM (B), 2 mM (C), 5 mM (D), and 10 mM (E) DTT for 7 h. The three peaks represent the P particle, the P dimer, and the degraded products (<10 kDa), respectively. (F and G) The same P particles were treated with 10% glycerol (F) or 50 mM Tris, pH 9 (G). (H and I) VLP of VA387 was treated by 1 mM (H) or 10 mM (I) DTT. The gel filtration column was calibrated using the same calibration kit as described in the legend to Fig. 1.

indicates that the hinge inhibited P particle formation. In separate studies, we have observed that addition of a small peptide to the ends of the P domain greatly affected the receptor binding of the P protein (Table 2). Since P particle formation also affects the receptor binding of the P protein (see below), we tested the effects of these peptides on the formation of the P particle of VA387. The first peptide tested contained five amino acids (CNGRC), a ligand of CD13 (aminopeptidase) found in tumor blood vessels (7, 27). Addition of this peptide to either the N or the C terminus of the H/P mutant resulted in nearly exclusive formation of the P particle (Fig. 2D and E).

When the NGR or QNGR motifs without cysteine were fused to the N terminus of H/P mutants, the P proteins formed dimer only (compare Fig. 2A and B to Fig. 2D and E). However, when one or more cysteines were added back to the peptides, the P proteins mainly formed P particles (Fig. 2C, F, G, H, and I). These data indicate that the cysteine, but not the NGR motif, was important for promoting P-particle formation. A single cysteine is probably sufficient for this promotion, as more cysteines only resulted in slight increase of the P particle formation (compare Fig. 2C to Fig. 2D to G). The CNGRC motif also promoted P particle formation of NV, a GI norovirus (compare Fig. 1B to Fig. 2J), although the efficiency was lower than that of VA387. This promotion effect was P protein specific, as fusion of CNGRC to the C terminus of the MBP (42 kDa) resulted only in aggregates of the protein with variable sizes (Fig. 2L and M). A fusion of the GST tag to the H/P mutant did not result in P particle formation either (Fig. 2K).

The cysteine-promoted P particle was sensitive to dithiothreitol (DTT) treatment at concentrations of 1 to 2 mM (Fig. 3A to C), indicating that an intermolecular disulfide bond is involved in the formation of the P particle. However, a further increase of DTT concentration (from 5 to 10 mM) did not lead to complete dissociation of the P particle (Fig. 3D and E), suggesting that forces other than a disulfide bond may also be involved in P particle formation. The disulfide bond may also play a role in P dimer and VLP formations, because degradations of these molecules have been observed following treatment with DTT in a dose-dependent manner (Fig. 3A to E, H, and I). In contrast, treatment of 10% glycerol or 50 mM Tris at pH 9 did not result in degradation of the P particle (Fig. 3F and G).

**The P particle revealed a unique morphology under EM.** We examined the FPLC-purified P particle by a negative staining EM. As shown in Fig. 4A and B, the P particles revealed ring- or pentagon-shaped structures with a diameter of ~5 nm, indicating that they are closed, spherical particles with a cavity inside. The P protein from the dimer fractions did not reveal these structures (data not shown).

**The P particle displays an enhanced ability to bind to HBGA receptors.** In our previous studies, we demonstrated that the P dimers bound to HBGAs but that the binding affinity was lower than that of the intact capsid (32). To determine if the P particle formation affects the receptor binding of the P proteins, we compared the P particles and the P dimers from the gel filtrations for receptor-binding activity. The results showed that the P particles of both VA387 and NV bound significantly

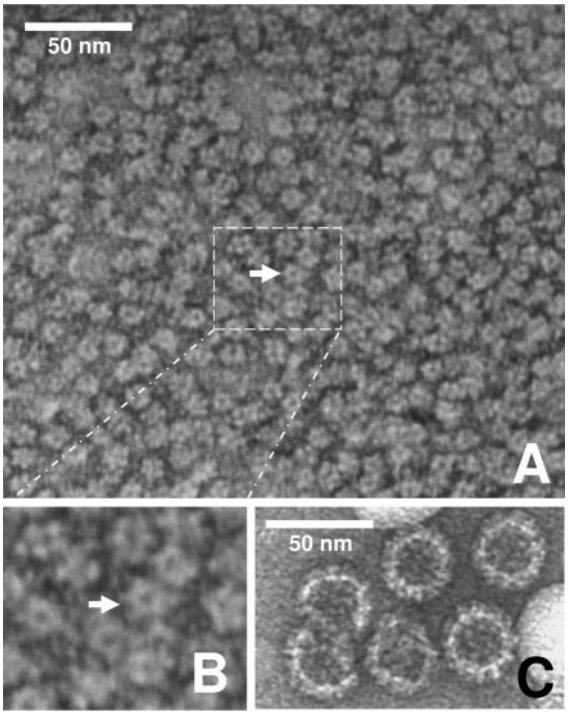


FIG. 4. Electron micrographs of negatively stained P particle. (A) FPLC-purified P particle of the H/P-CDCRGDCFC mutant of VA387. Arrows indicate a typical pentagon-ring structure of the P particle. The central part of panel A is enlarged in panel B. (C) Sucrose gradient-purified VA387 VLPs shown at the same magnification as in panel A.

more strongly than the P dimers by the saliva-based assays (Fig. 5). We then performed a systematic comparison of receptor-binding sensitivities of different mutant capsids (Table 2), which basically confirmed the conclusion of higher binding sensitivities of the P particles than the P dimers. The estimated binding sensitivity of the VA387 P particle to the B antigen was ~725-fold higher than that of the P dimers, even higher (~2-fold) than that of the VLPs. Similar binding enhancement was also observed with NV P particles, although the increase was less (81 fold for the A antigen). It was noted that binding enhancement to the A/B epitopes was significantly higher than to the H epitope for the VA387 P particle. This suggests that A/B and H are independent epitopes and that the VA387 P particles did not have a proper conformation for the H epitope. This is consistent with the norovirus receptor-binding model proposed recently by Huang et al. (17), in which the receptor-binding interface of the capsid possesses different sites interacting with the A/B and the H epitopes, respectively.

To further determine the role of the structural integrity of the capsid in receptor binding, we performed binding assays using different forms of the capsid, following a partial dissociation of VLPs. Two peaks of the capsid proteins were obtained from gel filtrations, following the treatments of VA387 VLPs with Tris buffer at pH 9.0 (36), which corresponded to the intact VLPs and the capsid protein dimers, respectively (Fig. 6A and B, left panels). A potential capsid intermediate, the pentamer of the capsid protein dimer, as suggested by Prasad et al. (28), was also observed when the VLPs in sucrose were treated with the Tris buffer (Fig. 6D). Receptor-binding assays revealed that the binding sensitivities of the dimers and the pentamers of dimers were significantly lower than those of the VLPs (Fig. 6B and D, right). Similar results also were obtained for NV VLPs (Fig. 6C). These data indicate that proper conformation of the capsid and/or the binding interface is important for receptor binding.

**The binding enhancement requires the authentic binding interface.** This conclusion was made from a study of a VA387 H/P mutant whose binding ability was destroyed by a single amino acid mutation ($T_{338}A$) at the receptor-binding interface (32, 33). Addition of the CNGRC motif to this mutant resulted in P particle formation (Fig. 7A to C) but did not restore the receptor-binding function of this mutant (Fig. 7D and E).

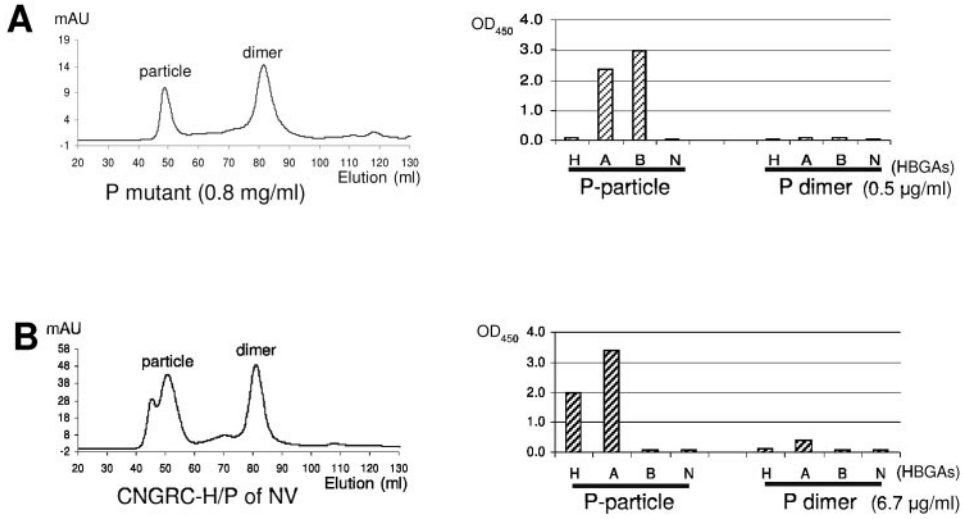


FIG. 5. The P particle displays enhanced binding to HBGAs. (A and B) Chromatographs of gel filtrations showing two peaks representing the P particle and the P dimer, respectively, of the P mutant of VA387 (A, left) and the CNGRC-H/P mutant of NV (B, left). Their binding activities to HBGAs were revealed on the right panels. H, A, B, and N stand for the saliva samples with blood types O, A, B, and nonsecretor, respectively.

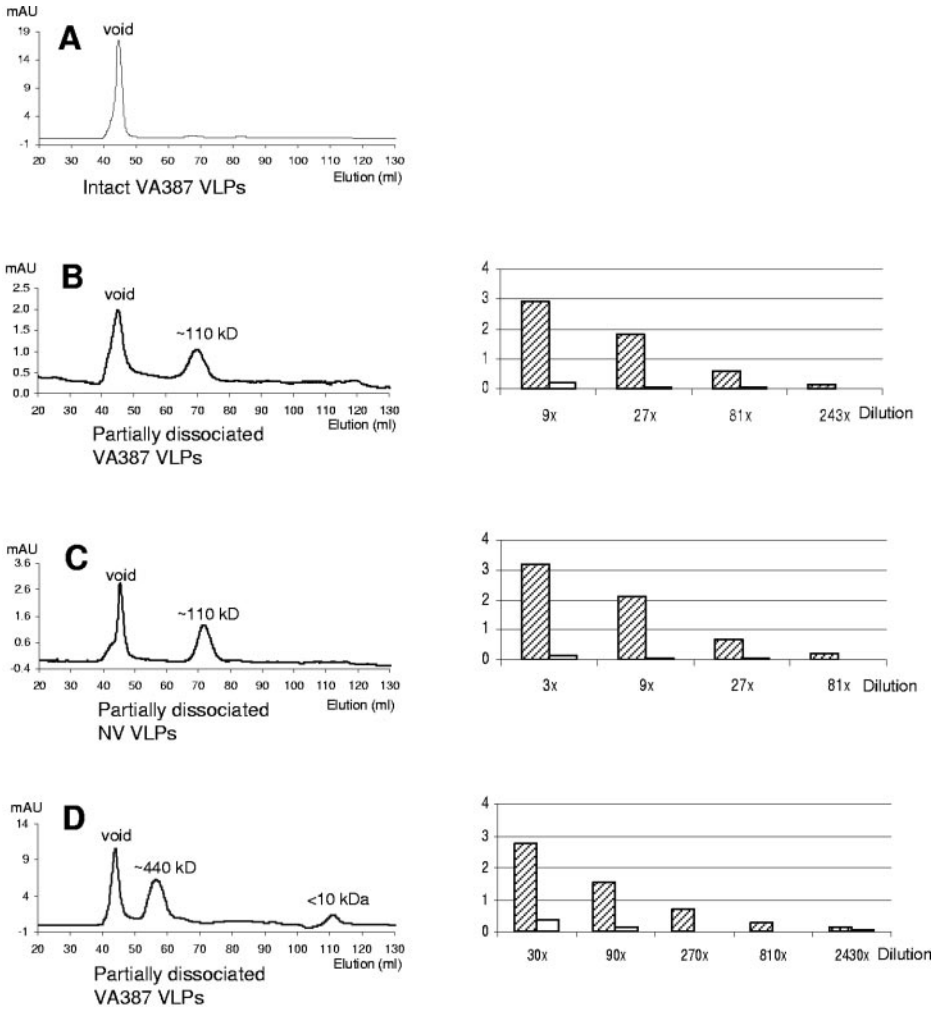


FIG. 6. The receptor-binding activities of VLP and its dissociated intermediate. (A) Gel filtration chromatograph of sucrose gradient-purified VA387 VLPs in PBS shows a single peak in the void volume. (B to D) Gel filtrations of partially dissociated VLPs of VA387 (B and D, left) and of NV (C, left) by 50 mM Tris, pH 9 (B and C), or by 50 mM Tris containing 30% sucrose (pH 9) (D), showing peaks representing the intact capsid (void), the potential pentamer of dimer (~440 kDa), capsid protein dimer (~110 kDa), and degraded product (<10 kDa), respectively. For each gel filtration, the peak fractions were collected and adjusted to the same protein concentration according to the UV reading. The resulting proteins then were used for binding assays, followed by a serial of threefold dilution (right). The striped columns show the binding of intact VLP, while the open columns show the binding of the dissociated intermediate to type A saliva. Data were averages of an experiment performed in triplicate.

**The P particle binds to human intestinal Caco-2 cells.** The enhanced receptor-binding activity of the P particle was also demonstrated in vivo using human colon carcinoma Caco-2 cells. Differentiated Caco-2 cells express H antigen (26), and they revealed specific binding to VA387 P particles (CNGRC-H/P) (Fig. 8, 1A to 2B). In contrast, the P dimers of the H/P mutant and the PC-5 (a HBGA-binding defective mutant) (Tan and Jiang, unpublished) did not reveal any binding (Fig. 8, 3A to 4B). The P particle binding only to a portion of the cell population indicates that the cells may be in different stages of differentiation with variable levels of HBGA expression.

## DISCUSSION

In this study, we demonstrated that the isolated capsid P protein of VA387 spontaneously forms a small particle with a unique morphology. Based on the molecular mass (~830 kDa), the shape (round and empty), the size (~5 nm in diameter), the dynamic of the P particle, as well as information from the literature (see below), we predicted that the P particle is a T=1 icosahedron. The molecular weight of the P particle suggested that it contains 24 P monomers organized into 12 identical P dimers (Fig. 9) (32). "Twelve" is a perfect unit number for an icosahedral symmetry that occurs frequently in other plant and animal viruses (15). In fact, when 12 ping-pong balls were put into a sack with slight pressing and twisting, a perfect T=1 icosahedron was formed (Fig. 9). Structural study of the Grimsby virus, a strain genetically closely related with VA387, revealed a spherical structure of the P dimer moiety in a capsomer (4), suggesting that the isolated P dimer is a spherical structure that fits easily in an icosahedral particle (15). The single peak of the P particle in gel filtrations indicates that the P proteins must be arranged into a low-energy order, consis-

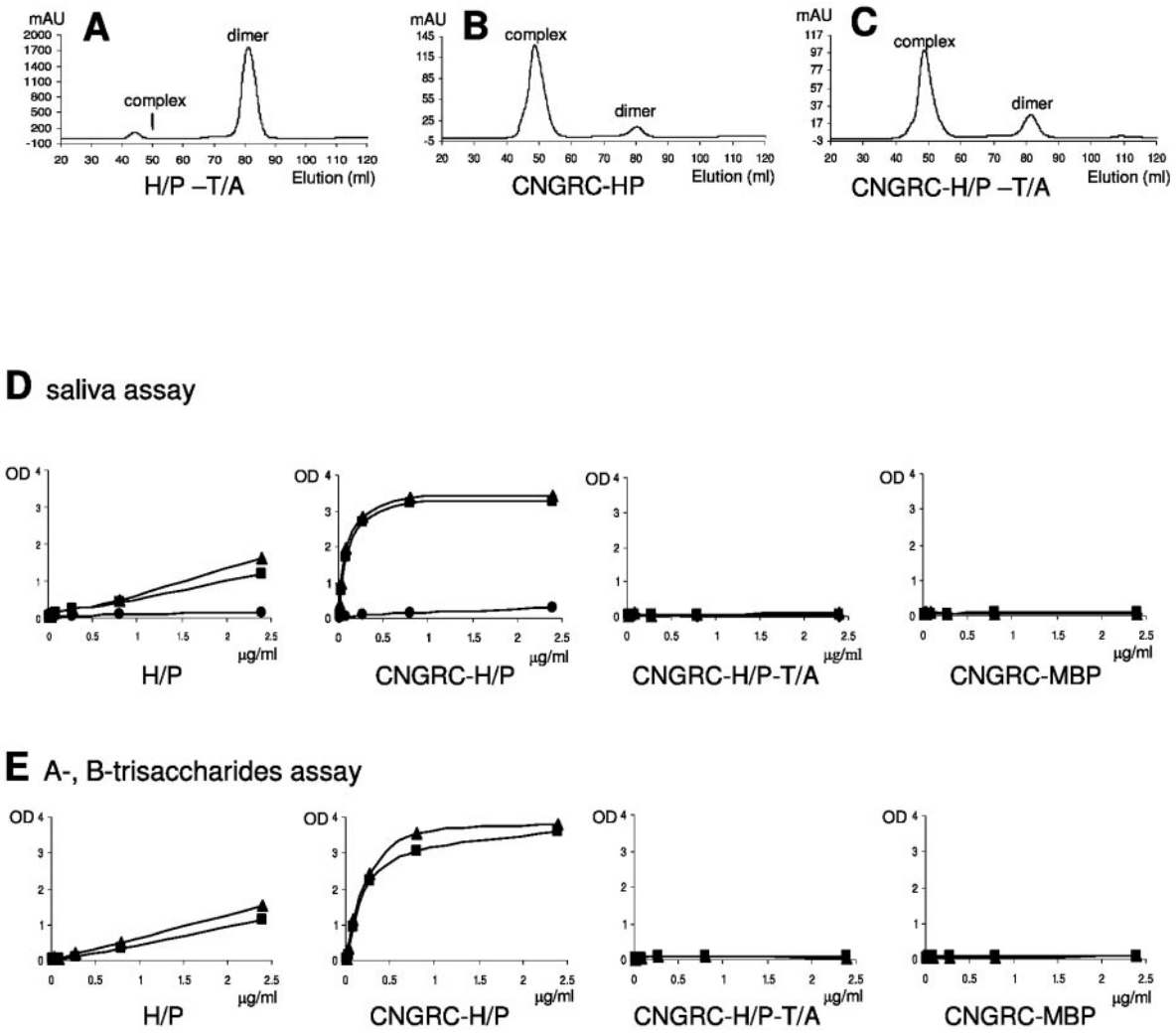


FIG. 7. The binding enhancement of the P particle requires the authentic binding interface. (A to C) Gel filtration chromatographs of the mutants H/P-T/A (A), CNGRC-H/P (B), and CNGRC-H/P-T/A (C), indicating that the mutation $T_{338}A$ does not affect P particle formation of the CNGRC-H/P mutant. (D and E) Binding curves of H/P, CNGRC-H/P, CNGRC-H/P-T/A, and CNGRC-MBP to saliva of O, A, B, and nonsecretor blood types (D) or to synthetic A- and B-trisaccharide–bovine serum albumin conjugate (E). The data for binding curves are mean values of triplicate experiments. Saliva types: ■, A; ▲, B; and ●, O.

tent with the property of an icosahedron. The same T=1 icosahedral structure with 12 pentamers of N-terminally truncated capsid proteins in human papillomavirus has been reported (5). In addition, a number of studies on other plant and animal viruses have also demonstrated T=1 subviral particles from truncated capsid proteins (1, 6, 8, 24, 30). Thus, the formation of subviral particles by truncated viral capsid proteins is a common phenomenon.

To summarize the available data, we propose the following model to explain the dynamic of the P particle formation (Fig. 9). There are probably only two forms of P proteins in existence: the P dimer and the P particle. The P monomer must instantly form dimers after their expression or releasing from the GST tag by thrombin digestion, because we never saw P monomer in the gel filtration experiment. The P dimers have a high potential to assemble into P particles, a possible intrinsic feature of the capsid protein in the capsid formation. The P dimers and the P particles can exchange dynamically, depending on P protein concentrations. As a matter of fact, 7 of the 10 putative intermolecular interactive sites of the capsid protein are located in the P domain, according to the atomic structure of the NV capsid (28). Thus, there must be multiple dimerization or polymerization interactions in the P domain that are responsible for the P dimer, the P particle, and VLP formations. Additions of cysteines at the ends of the P protein clearly favor these interactions and P particle formation. Although it is not clear how each P monomer is orientated in individual P dimers, all P dimers should have the same orientation in their interaction with the five surrounding P dimers (Fig. 9). Since the P2 subdomain is known to be responsible for receptor binding, the outer layer of the P particle must be formed by the P2 subdomain, similar to that on the norovirus VLPs (4, 28), while the inner layer is made by the P1 subdomain, providing support to the P2 tip. We predict that the P particle is an empty

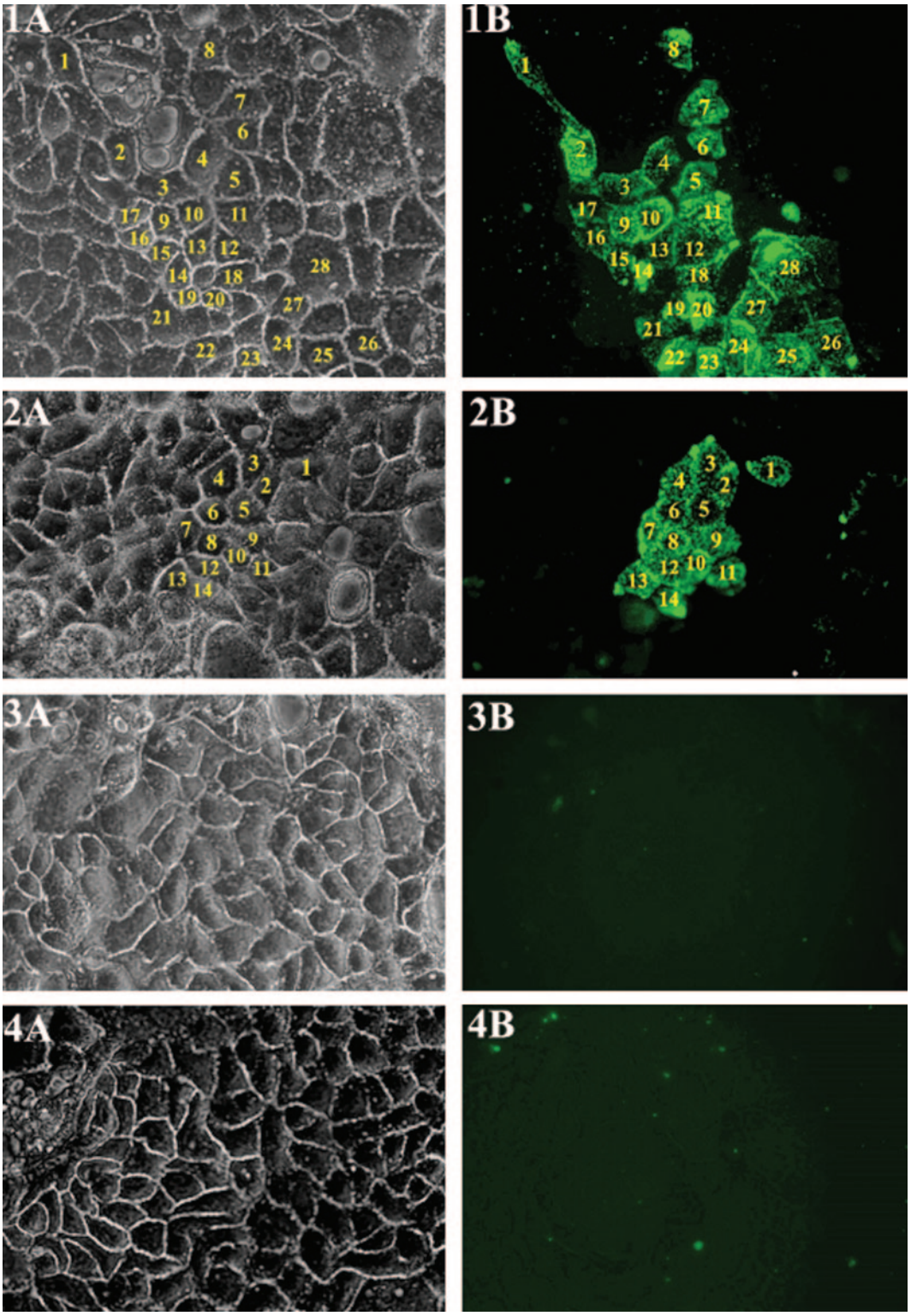


FIG. 8. The P particle of VA387 binds to differentiated Caco-2 cells. The left panels are phase-contrast micrographs of the differentiated Caco-2 cells after incubation with the biotinylated P particles (CNGRC-H/P) and P dimers (H/P or PC-5). The nonbinding mutant (PC-5) (Tan and Jiang, unpublished) served as a negative control. The cell-bound P proteins were detected with fluorescein isothiocyanate-streptavidin (Pierce) observed by fluorescence microscopy (right panels). Cells were 10 days after confluence. Micrographs in both panels show the same fields of the cell cultures. The yellow numbers indicate the cells bound by the P particle.

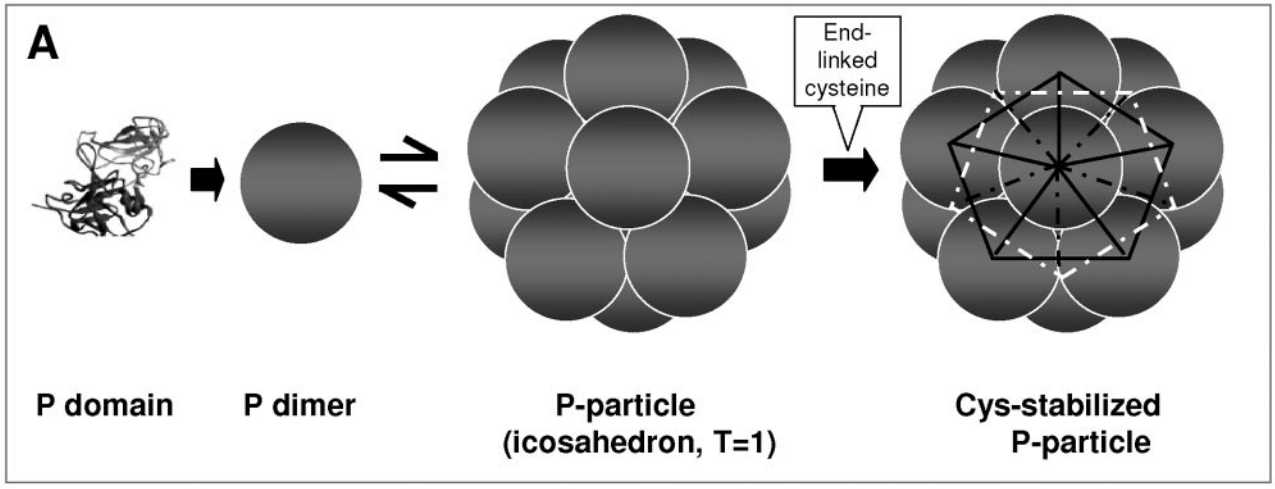


FIG. 9. A model of P particle formation. (A) Steps of P particle formation. P monomers spontaneously form a globular P dimer. Then, 12 identical P dimers assemble into a T=1 icosahedral P particle (P protein concentration dependent). The intermolecular interactions among the P domains are the original forces for P particle formation. An end-linked cysteine(s) stabilizes the P particle by forming intermolecular disulfide bonds. See the text for details. (B) Comparison of the cross-section of the proposed P particle with the enlarged EM image of the P particle.

particle, based on the ring-like structure of the particles seen by EM (Fig. 9B). Direct evidence for this prediction requires cryo-EM or crystallography studies.

It becomes understandable based on the proposed model of the P particle why the presence of the hinge inhibits P particle formation. In VLPs, the hinge must provide a limited freedom to the P domain for the icosahedral capsid structure in the presence of the S domain (28). In the P particle, however, such freedom is no longer required because of the absence of the S domain. Therefore, the presence of the hinge becomes an extra plug interrupting P1-P1 interactions. In contrast, the P1-linked cysteine(s) strengthens the P1-P1 interaction by disulfide bonds.

It has been shown that the N-terminal region of the capsid protein of many plant and animal viruses contain a molecular switch controlling the conformation of the icosahedral capsid. When such switch was deleted from the rabbit hemorrhagic disease virus, an animal calicivirus, the mutant capsid protein formed a T=1 icosahedral particle (1). This molecular switch is more common in plant viruses. When the N-terminal arms of the capsid protein were removed, the mutant capsids of many plant viruses assembled into T=1 particles (6, 8, 24, 30). However, additional mechanisms may also exist: the NV mutant lacking the N-terminal arm is able to assemble into a T=3 capsid (2), while both T=1 and T=3 particles could be observed when the NV full-length capsid protein was expressed in insect cells (36). Thus, the P particle described here may represent only one consequence of many potential intermolecular interactions. A further question would be whether these T=1 particles are biologically relevant.

The finding of a large amount of soluble P domain in the stools of norovirus-infected patients (11, 12) indicates a favorable answer to the above question of the biological relevance of the P protein. One potential function is that the P protein may serve as a decoy for the progeny virions to escape host immunity (12). Such P protein might result from the proteolytic digestion of the capsid protein at the junction between the S and the P domains. The highly conserved trypsin digestion site in many noroviruses (12) implies a potential evolutionary selection. The fact that only the P domain survives in the intestine indicates that the P protein must be well folded so that it is resistant to proteolytic digestions. To determine whether the P protein forms P particles in vivo, we performed gel filtration analyses of the P protein of stools of norovirus-infected patients. The results revealed signals in fractions corresponding to the P particles and the P dimers (Tan and Jiang, unpublished). However, further experiments to confirm the results require collection of a large volume of clinical samples.

The most important observation of this study is the significant enhancement of binding affinity of the P particle to HBGAs compared with that of the P dimer. The increased receptor-binding sites of the P particle compared with those of the P dimers could be the major factor for the enhancement. The even higher binding sensitivity of the P particle than that of VLP (Table 2) may be due to increased binding units of the P particles compared with that of the VLPs ($M_r$ = 10.4 mDa), as ~2-fold increases in binding sites in the P particles over VLPs are expected in a given amount of proteins. As mentioned earlier, however, the binding enhancement of the P particle to the H epitopes was different between different strains. Little enhancement was observed for VA387, while significant enhancement was observed for the NV P particle (Fig. 2 and Table 2). More interestingly, when a cysteine-

containing motif, CGAGC, was linked to the C terminus of the P domain of VA387, the resulting P particles revealed a strong binding to saliva of all A, B, H, and nonsecretor blood types (Tan and Jiang, unpublished). Thus, the mechanism of the enhancement is complicated. In addition to the receptor-binding interface, the conformation of the surrounding regions and possibly the overall structure of the P particles also play a role in binding sensitivity and specificity.

The facts that the P particle binds strongly to human intestinal Caco-2 cells (Fig. 8) and that the P particle of VA387 (a GII strain) cross blocked the binding of NV VLP (a GI strain) to HBGAs (Tan and Jiang, unpublished) suggest that the P particle could be used as a decoy receptor to treat norovirus infection. Although we are unable to demonstrate blocking among many strains, due to the lack of the specific antibody, it seems logical to predict the existence of blocking among homologous strains between P particle and virions. The easy production of the cysteine-stabilized P particle and the survival of the P protein through the intestinal tract make this strategy more attractive. In addition, the P particle may serve as a vaccine for an extended protection following this treatment. In a separate study, we observed that administration of VA387 P proteins to mice intranasally produced specific antibody that can block the binding of VA387 to HBGAs (Tan and Jiang, unpublished).

Using two different buffer conditions, we were able to dissociate the norovirus VLPs into two types of intermediates: the capsid protein dimer (~116 kDa) and the pentamer of dimers (~580 kDa) (Fig. 6). Based on the crystal structure of the NV capsid, Prasad and coworkers (28) proposed a capsid assembly pathway, in which the capsid protein monomers first form dimers, and then the dimers polymerize into a pentamer of dimers, which then further assemble into icosahedral capsids. To our knowledge, our data are the first experimental findings supporting the proposed assembly pathway.

## ACKNOWLEDGMENTS

We thank Yang Bai, Brad Jennings, and Dan Song for technical support for this study and Tibor Farkas for critical reading of the manuscript.

The research described in this article was supported by the U.S. National Institutes of Health (National Institute of Allergy and Infectious Diseases, grant RO1 AI37093-7, and National Institute of Child Health and Human Development, grant HD13021) and the Department of Defense (DoD grant PR033018).

## REFERENCES

1. **Barcena, J., N. Verdaguer, R. Roca, M. Morales, I. Angulo, C. Risco, J. L. Carrascosa, J. M. Torres, and J. R. Caston.** 2004. The coat protein of rabbit hemorrhagic disease virus contains a molecular switch at the N-terminal region facing the inner surface of the capsid. Virology **322:**118–134.
2. **Bertolotti-Ciarlet, A., L. J. White, R. Chen, B. V. Prasad, and M. K. Estes.** 2002. Structural requirements for the assembly of Norwalk virus-like particles. J. Virol. **76:**4044–4055.
3. **Chakravarty, S., A. M. Hutson, M. K. Estes, and B. V. Prasad.** 2005. Evolutionary trace residues in noroviruses: importance in receptor binding, antigenicity, virion assembly, and strain diversity. J. Virol. **79:**554–568.
4. **Chen, R., J. D. Neill, J. S. Noel, A. M. Hutson, R. I. Glass, M. K. Estes, and B. V. V. Prasad.** 2004. Inter- and intragenus structural variations in caliciviruses and their functional implications. J. Virol. **78:**6469–6479.
5. **Chen, X. S., R. L. Garcea, I. Goldberg, G. Casini, and S. C. Harrison.** 2000. Structure of small virus-like particles assembled from the L1 protein of human papillomavirus 16. Mol. Cell **5:**557–567.
6. **Cuillel, M., B. Jacrot, and M. Zulauf.** 1981. A T=1 capsid formed by protein of brome mosaic virus in the presence of trypsin. Virology **110:**63–72.
7. **Curnis, F., G. Arrigoni, A. Sacchi, L. Fischetti, W. Arap, R. Pasqualini, and A. Corti.** 2002. Differential binding of drugs containing the NGR motif to CD13 isoforms in tumor vessels, epithelia, and myeloid cells. Cancer Res. **62:**867–874.
8. **Erickson, J. W., A. M. Silva, M. R. Murthy, I. Fita, and M. G. Rossmann.** 1985. The structure of a T = 1 icosahedral empty particle from southern bean mosaic virus. Science **229:**625–629.
9. **Fankhauser, R. L., S. S. Monroe, J. S. Noel, C. D. Humphrey, J. S. Bresee, U. D. Parashar, T. Ando, and R. I. Glass.** 2002. Epidemiologic and molecular trends of "Norwalk-like viruses" associated with outbreaks of gastroenteritis in the United States. J. Infect. Dis. **186:**1–7.
10. **Glass, R. I., J. Bresee, B. Jiang, J. Gentsch, T. Ando, R. Fankhauser, J. Noel, U. Parashar, B. Rosen, and S. S. Monroe.** 2001. Gastroenteritis viruses: an overview. Novartis Found. Symp. **238:**5–19.
11. **Greenberg, H. B., J. R. Valdesuso, A. R. Kalica, R. G. Wyatt, V. J. McAuliffe, A. Z. Kapikian, and R. M. Chanock.** 1981. Proteins of Norwalk virus. J. Virol. **37:**994–999.
12. **Hardy, M. E., L. J. White, J. M. Ball, and M. K. Estes.** 1995. Specific proteolytic cleavage of recombinant Norwalk virus capsid protein. J. Virol. **69:**1693–1698.
13. **Harrington, P. R., L. Lindesmith, B. Yount, C. L. Moe, and R. S. Baric.** 2002. Binding of Norwalk virus-like particles to ABH histo-blood group antigens is blocked by antisera from infected human volunteers or experimentally vaccinated mice. J. Virol. **76:**12335–12343.
14. **Harrington, P. R., J. Vinje, C. L. Moe, and R. S. Baric.** 2004. Norovirus capture with histo-blood group antigens reveals novel virus-ligand interactions. J. Virol. **78:**3035–3045.
15. **Harrison, S. M.** 2001. Principles of virus structure, p. p. 53–86. *In* D. M. Knipe P. M. Howley, D. E. Griffin, R. A. Lamb, M. A. Martin, B. Roizman, and S. E. Straus (ed.), Fields virology, 4th ed. Lippincott Williams & Wilkins, Philadelphia, Pa.
16. **Huang, P., T. Farkas, S. Marionneau, W. Zhong, N. Ruvoen-Clouet, A. L. Morrow, M. Altaye, L. K. Pickering, D. S. Newburg, J. LePendu, and X. Jiang.** 2003. Noroviruses bind to human ABO, Lewis, and secretor histo-blood group antigens: identification of 4 distinct strain-specific patterns. J. Infect. Dis. **188:**19–31.
17. **Huang, P. W., T. Farkas, W. M. Zhong, M. Tan, S. Thornton, A. L. Morrow, and X. Jiang.** 2005. Norovirus and histo-blood group antigens: demonstration of a wide spectrum of strain specificity and classification of two major binding groups among multiple binding patterns. J. Virol. **79:**6714–6722.
18. **Hutson, A. M., R. L. Atmar, and M. K. Estes.** 2004. Norovirus disease: changing epidemiology and host susceptibility factors. Trends Microbiol. **12:**279–287.
19. **Hutson, A. M., R. L. Atmar, D. M. Marcus, and M. K. Estes.** 2003. Norwalk virus-like particle hemagglutination by binding to H histo-blood group antigens. J. Virol. **77:**405–415.
20. **Hutson, A. M., S. Charkravarty, R. L. Atmar, B. V. Prasad, and M. Estes.** 2004. Loss of carbohydrate binding with point mutations of Norwalk virus virus-like particles. Second International Calicivirus Conference, Dijon, France, 6–10 November, 2004.
21. **Jiang, X., M. Wang, D. Y. Graham, and M. K. Estes.** 1992. Expression, self-assembly, and antigenicity of the Norwalk virus capsid protein. J. Virol. **66:**6527–6532.
22. **Lindesmith, L., C. Moe, J. Lependu, J. A. Frelinger, J. Treanor, and R. S. Baric.** 2005. Cellular and humoral immunity following Snow Mountain virus challenge. J. Virol. **79:**2900–2909.
23. **Lindesmith, L., C. Moe, S. Marionneau, N. Ruvoen, X. Jiang, L. Lindblad, P. Stewart, J. LePendu, and R. Baric.** 2003. Human susceptibility and resistance to Norwalk virus infection. Nat. Med. **9:**548–553.
24. **Lokesh, G. L., T. D. Gowri, P. S. Satheshkumar, M. R. Murthy, and H. S. Savithri.** 2002. A molecular switch in the capsid protein controls the particle polymorphism in an icosahedral virus. Virology **292:**211–223.
25. **Marionneau, S., A. Cailleau-Thomas, J. Rocher, B. Le Moullac-Vaidye, N. Ruvoen, M. Clement, and J. Le Pendu.** 2001. ABH and Lewis histo-blood group antigens, a model for the meaning of oligosaccharide diversity in the face of a changing world. Biochimie **83:**565–573.
26. **Marionneau, S., N. Ruvoen, B. Le Moullac-Vaidye, M. Clement, A. Cailleau-Thomas, G. Ruiz-Palacois, P. Huang, X. Jiang, and J. Le Pendu.** 2002. Norwalk virus binds to histo-blood group antigens present on gastroduodenal epithelial cells of secretor individuals. Gastroenterology **122:**1967–1977.
27. **Pasqualini, R., E. Koivunen, R. Kain, J. Lahdenranta, M. Sakamoto, A. Stryhn, R. A. Ashmun, L. H. Shapiro, W. Arap, and E. Ruoslahti.** 2000. Aminopeptidase N is a receptor for tumor-homing peptides and a target for inhibiting angiogenesis. Cancer Res. **60:**722–727.
28. **Prasad, B. V., M. E. Hardy, T. Dokland, J. Bella, M. G. Rossmann, and M. K. Estes.** 1999. X-ray crystallographic structure of the Norwalk virus capsid. Science **286:**287–290.
29. **Ravn, V., and E. Dabelsteen.** 2000. Tissue distribution of histo-blood group antigens. APMIS **108:**1–28.
30. **Savithri, H. S., and J. W. Erickson.** 1983. The self-assembly of the cowpea strain of Southern bean mosaic virus: formation of T=1 and T=3 nucleoprotein particles. Virology **126:**328–335.
31. **Tan, M., and X. Jiang.** 2005. Norovirus and its histo-blood group anti-

gen receptors: an answer to a historical puzzle. Trends Microbiol. **13:** 285–293.
32. **Tan, M., R. S. Hegde, and X. Jiang.** 2004. The P domain of norovirus capsid protein forms dimer and binds to histo-blood group antigen receptors. J. Virol. **78:**6233–6242.
33. **Tan, M., P. Huang, J. Meller, W. Zhong, T. Farkas, and X. Jiang.** 2003. Mutations within the P2 domain of norovirus capsid affect binding to human histo-blood group antigens: evidence for a binding pocket. J. Virol. **77:** 12562–12571.
34. **Tan, M., W. Zhong, D. Song, S. Thornton, and X. Jiang.** 2004. E. coli-expressed recombinant norovirus capsid proteins maintain authentic antigenicity and receptor binding capability. J. Med. Virol. **74:**641–649.
35. **White, L. J., J. M. Ball, M. E. Hardy, T. N. Tanaka, N. Kitamoto, and M. K. Estes.** 1996. Attachment and entry of recombinant Norwalk virus capsids to cultured human and animal cell lines. J. Virol. **70:**6589–6597.
36. **White, L. J., M. E. Hardy, and M. K. Estes.** 1997. Biochemical characterization of a smaller form of recombinant Norwalk virus capsids assembled in insect cells. J. Virol. **71:**8066–8072.